BIOMEDICAL ENGINEERING MSc PROGRAM
UNIVERSITY OF CRETE
TECHNICAL UNIVERSITY OF CRETE
FOUNDATION FOR RESEARCH AND TECHNOLOGY-HELLAS

Application Grade Thesis

Signal to Noise Ratio reproducibility measurements in clinical MRI examinations

Georgios Makris Tsalikis

Supervisor: Prof. Thomas G Maris

2nd member committee: Prof. Apostolos Karantanas

Date of completion: April of 2022

This dissertation is submitted as a partial fulfilment of the requirements for the Master's degree of Biomedical Engineering M.Sc. program

Διπλωματική Εργασία

Επαναληψιμότητα μετρήσεων λόγου σήματος πρός θόρυβο σε κλινικές εικόνες μαγνητικού συντονισμού.

Μακρής Τσαλίκης Γεώργιος

Επιβλέπων Καθηγητής: Θ. Μαρής

2ο Μέλος Επιτροπής : Α. Καραντάνας

Ημερομηνία ολοκλήρωσης : Απρίλιος 2022

Αυτή η διπλώματική κατατίθεται ως προαπαιτούμενη στα πλαίσια του ΠΜΣ Βιοατρική Μηχανική.

Acknowledgements

I would like to express my deepest gratitude to Professor Thomas G Maris and Professor Apostolos Karantanas for their guidance throughout this dissertation and for going in great lengths providing all the necessary means in order fulfill this research.

To my mentor in Magnetic Resonance Imaging Giakoumelos Alexios MSc Medical Physicist a special thank you for your constant support.

To all my fellow students on this program much appreciation for their help.

Much obliged to my spouse Stella for all the support and understanding during this difficult era.

Abstract

During this thesis we will attempt to evaluate the performance , in terms of SNR , of the equipment used for Magnetic Resonance Imaging of a brain by the homonymous department of the University Hospital of Herakleion. This procedure usually is part of a much larger Quality Assurance program but it the one that is repeated most frequently due to the fact that the SNR as metric is straight forward indicator of the image quality produced by the equipment.

This as a practice occupies valuable scantime that could be invested in patient care or forces medical physists and radiographers to perform the procedure after hours when the equipment is not in clinical use (if that time exists). Performing such a crucial procedure after a long day is an error prone procedure. A viable alternative solution could be a procedure that runs with the already acquired datasets and acts as an indicator of the system status and does not mandate the use of the equipment itself.

In order to evaluate the performance of the aforementioned equipment and hence feasibility of this alternative method of performance status monitoring (in terms of SNR measurement) we designed an image evaluation process that consists of nine areas of measurments (ROIs) one in the background area of the image and eight measurements in four specific areas of the imaged brain.
These four areas were selected carefully to meet certain criteria , to be in key areas of the brain that pathology is easily depicted in order to be excluded in such case and the areas should cover the center of the image but also the edges. By combining these eight brain measurements with the background measurement (that acts as a noise measurement) via the practical SNR measurement technique as described by the American Association of Physicists in Medicine (AAPM) will be having data tabulated that reflect the performance in actual conditions and not in ideal conditions that are used in the usual Quality Assurance program.

This image evaluation process was applied in a single T2 Fast Spin Echo image that was acquired during the scanning of a T2 FSE imaging series when routine brain protocol was used in longitudinal period of three years. The review of those images was performed retrospectively in Evorad PACS-HIS workstation and the statistical analysis of the data was performed under MedCalc software.

Thorough analysis of the data revealed consistent recurrence of values with no statistical difference between the sets of variables proving the stability of the imaging equipment during the inspected period of time and providing us with the initial data that we could be standing infront of a viable alternative method for SNR performance status monitoring if performed under certain circumstances.

Απόσπασμα

Κατά τη διάρκεια αυτής της διπλωματικής εργασίας θα επιχειρήσουμε να αξιολογήσουμε την απόδοση, ως προς το SNR, του εξοπλισμού που χρησιμοποιείται στην απεικόνιση μέσω Μαγνητικού Συντονισμού εγκεφάλου από το ομώνυμο τμήμα του Πανεπιστημιακού Νοσοκομείου Ηρακλείου. Αυτή η διαδικασία είναι συνήθως μέρος ενός πολύ μεγαλύτερου προγράμματος διασφάλισης ποιότητας, αλλά είναι αυτο το κομμάτι που επαναλαμβάνεται συχνότερα λόγω του γεγονότος ότι το SNR ως τιμή έχει ευθεία συσχέτιση με την ποιότητας εικόνας που παράγεται από τον εξοπλισμό.

Αυτό ως πρακτική καταλαμβάνει πολύτιμο χρόνο που θα μπορούσε να επενδυθεί στη φροντίδα των ασθενών ή αναγκάζει τους φυσικούς ιατρικής και τους τεχνολόγους ακτινολόγους να εκτελέσουν τη διαδικασία μετά από ώρες που ο εξοπλισμός δεν είναι σε κλινική χρήση (αν υπάρχει αυτός ο χρόνος. Μια βιώσιμη εναλλακτική λύση θα μπορούσε να είναι μια διαδικασία που εκτελείται με τα ήδη αποκτηθέντα σύνολα δεδομένων και λειτουργεί ως δείκτης της κατάστασης του συστήματος και δεν επιβάλλει τη χρήση του ίδιου του εξοπλισμού.

Προκειμένου να αξιολογηθεί η απόδοση του προαναφερθέντος εξοπλισμού και συνεπώς η σκοπιμότητα αυτής της εναλλακτικής μεθόδου παρακολούθησης της κατάστασης απόδοσης (όσον αφορά τη μέτρηση SNR), σχεδιάσαμε μια διαδικασία αξιολόγησης εικόνας που αποτελείται από εννέα περιοχές μετρήσεων (ROI) μία στην περιοχή φόντου της εικόνας και οκτώ μετρήσεις σε τέσσερις συγκεκριμένες περιοχές του απεικονιζόμενου εγκεφάλου.
Αυτές οι τέσσερις περιοχές επιλέχθηκαν προσεκτικά για να πληρούν ορισμένα κριτήρια, να βρίσκονται σε βασικές περιοχές του εγκεφάλου που η παθολογία απεικονίζεται εύκολα για να αποκλειστεί σε τέτοια περίπτωση και οι περιοχές να καλύπτουν το κέντρο της εικόνας αλλά και τις άκρες. Συνδυάζοντας αυτές τις οκτώ μετρήσεις εγκεφάλου με τη μέτρηση υποβάθρου (που λειτουργεί ως μέτρηση θορύβου) μέσω της πρακτικής τεχνικής μέτρησης SNR, όπως περιγράφεται από την Αμερικανική Ένωση Φυσικών στην Ιατρική (AAPM) θα έχουμε δεδομένα σε πίνακα που αντικατοπτρίζουν την απόδοση σε πραγματικές συνθήκες και όχι σε ιδανικές συνθήκες που χρησιμοποιούνται στο συνηθισμένο πρόγραμμα Διασφάλισης Ποιότητας.

Αυτή η διαδικασία αξιολόγησης εικόνας εφαρμόστηκε σε μία μόνο εικόνα T2 Fast Spin Echo που λήφθηκε κατά τη σάρωση μιας σειράς απεικόνισης T2 FSE όταν χρησιμοποιήθηκε πρωτόκολλο ρουτίνας εγκεφάλου σε ρονική περίοδο τριών ετών. Η ανασκόπηση αυτών των εικόνων πραγματοποιήθηκε αναδρομικά στον σταθμό εργασίας Evorad PACS-HIS και η στατιστική ανάλυση των δεδομένων πραγματοποιήθηκε στο λογισμικό MedCalc.

Table of contents

Table of Contents

List of figures

List of tables

Chapter 1: Introduction

During this thesis we will investigate the behaviour, over time, of the equipment used in clinical MR imaging located at the facilities of University hospital of Heraklion, through multiple series of repetitive measurements on clinical MR images that have already been captured during exams that were performed over a three year span (2018-2020) in the solely MR scanner of the University hospital of Heraklion.

In order one to have a better understanding over the project, should be familiar some key concepts such as:

- Basic magnetic resonance definitions (TR, TE, Flip Angle)
- How signal is produced in MR imaging.
- What is T1 and T2 relaxation times?
- The three parent MR image contrast categories.
- What is SNR in MR imaging.

A short explanation will be provided over these concepts in order to better conceptualise the tasks performed throughout the project.

Basic physics and production of signal in MR imaging

Basic physics states that atoms consist of electrons orbiting a central nucleus composed of neutrons and protons, and electrons, protons and neutrons are known as fundamental particles. Magnetic resonance imaging originates from nuclear magnetic resonance, from that it is quite clear that we only focus in the nucleus. Specifically we need to look at the nucleus of the hydrogen atom, because it's abundant in the human body in water and other molecules. The nucleus of the hydrogen atom is a solely positively charged proton.

All fundamental particles spin on their own axis, consecutively hydrogen nucleus is constantly rotating positive charge. Fundamental electromagnetism tells us that a moving charge has an associated magnetic field, and so the proton generates its own tiny field known as its magnetic moment. If the proton is placed in a strong external magnetic field (static magnetic field of an MR scanner in our case), it is forced to align with the direction of the static field. The proton attempts to align with static magnetic field, but due to quantum mechanics laws this is partially accomplished. If we apply some quantum mechanics we will understand why the protons don't simply align with the field, but through classical mechanics it is possible to explain almost everything else.

Since protons do not align exactly with the static field, they continue to experience a torque which makes it them precess around the direction of the field. This precession is analogous to the wobbling of a spinning wheel tilted slightly off axis so that it experiences a torque due to gravity. The precessional frequency of the protons is found to be proportional to the external magnetic field, given by the Larmor equation. So the protons in a magnetic field all precess at the same Larmor frequency. This is known as a resonance condition.

In the already excited the protons if we apply an external RF pulse this will flip them out of their (partial) alignment for as long the pulse lasts. When the RF is switched off, they begin to return back to their equilibrium position. There are two main characteristics of the relaxation: the de-phasing of the spins following their phase coherence after the pulse, and re-alignment along their axis as they lose the energy they absorbed from the pulse. Simplistically speaking this energy release is captured as a signal through a readout equipment known as receive coil and transformed into an actual image.

This far we have explained simplistically the concepts under signal is created i.e. static magnetic field, RF pulses. But what about spatial information? How do we know which signal is coming from where? This is where another key component (gradient coils) take part by creating an alternating gradient field and by generating gradient pulses, these are generated in order to acquire spatial information about the area being imaged.

Images are created, as already described, using pulse sequences. These sequences are series of radiofrequency pulses and gradient pulses which their creation relies on the selection the operator does on specific timing parameters. The alternating gradient pulses make the peculiar noise resembling a person tapping on a wooden when the scanner is operational.

There are two main ‘families’ of sequences spin echo (SE) and gradient echo (GRE) , everything else is derived from these two, but they all have timing values called TR, and TE, which the operator sets accordingly in order to acquire the desired image contrast.

Repetition Time (TR) is the period between the applications of the excitation pulse to the application of the next pulse. This defines how much longitudinal magnetization recovers between each pulse. It is measured in milliseconds.[1]

Echo Time (TE) refers to the period between the application of the radiofrequency excitation pulse and the peak of the signal induced in the coil. It is measured in milliseconds. The amount of T2 relaxation is controlled by the TE.[2]

Flip angle is phenomenon under which the axis of the hydrogen proton deflects from its longitudinal plane axis z (parallel to the lines of the static magnetic field) to its transverse plane XY axis by excitation with the help of radiofrequency (RF) pulses. The RF pulse is sent in at the precise Larmor frequency in relation to the gyromagnetic ratio and magnetic field strength.

Magnetic resonance imaging take advantage of the properties hydrogen has which, as part of water or lipids, makes up to 75–80% of the human body. The most important properties are the proton density (often mentioned as PD), and two distinct times called spin-lattice relaxation time(T1 relaxation time) and spin-spin relaxation time(T2 relaxation time). Proton density is binded to the number of hydrogen atoms in a specific volume. Relaxation times describe how long the tissue takes to get back to equilibrium after an RF pulse. T1 and T2 depend on the different tissues, fluids have long T1 relaxation time, water rich tissues are usually in an intermediate range, and tissues rich in fat generally have short T1 relaxation time. T2 is always shorter than T1 for a given tissue. Fluids have the longest T2 relaxation time, while water rich tissues tend to have longer T2 relaxation than fat rich tissue.[3]

Generally images have contrast which depends on either PD, T1 or T2. In PD images, high proton densities give high signal values which corresponds in bright pixels on the image. In T2 weighted images, tissues with long T2 give the highest signal intensities, producing high signal translating into bright areas. T1 weighted images are a different story, long T1 tissues give the weakest signal (due to de-phasing outside of the echoing time (TE), meaning that bright pixels on T1 are associated with short T1 relaxation time.

TR		TE	
		Short	Long
		less than 40ms	More than 75ms
Short	(less than 750ms)	T1 weight	intermediate confusing state not in use
Long	(bigger than 750ms)	PD weight	T2 weight

Table 1. Spin Echo TR and TE timings for T1, T2 and PD images.

As mentioned before there are two families of pulse sequences, called spin echo and gradient echo, Spin Echo sequences use two RF pulses to create the echo which measures the signal intensity. Spin Echo can produce T1, T2, or PD weighted images depending on the tuning of TR and TE as shown in the previous table. Spin Echo sequences generally produce better quality images but scanning them

last longer. Gradient Echo sequences use a single RF pulse followed by a gradient pulse to create the echo, which also measures the signal intensity. Gradient Echo can produce T1, T2 or PD images (according to timings shown on table 2) and have much shorter TRs than SE, so they need less time to scan.

Flip Angle		TE	
		Short	Long
		less than 15ms	More than 30ms
Small	smaller than 40◦	PD weight	T2 weight
Long	bigger than 50◦	T1 weight	intermediate confusing state not in use

Table 2. Gradient Echo sequence timings.

MR image contrast categories:

T1

T1 weighted images can be generated using either the SE or the GE sequence. For Spin Echo imaging we need to use a short TR and a short TE to enhance the T1 differences between tissues. T1-weighted images have excellent contrast: fluids are dark (except when they flow through the imaging volume), water based structures are greyish and fat based structures are very bright. They are often known as 'anatomy scans', as they depict clearly the boundaries between tissues. [4]

T2

T2 weighted contrast images can be produced by Spin Echo or Gradient Echo sequences, but Gradient Echo image implementation is tricky because these sequences are heavily affected by any magnetic field in homogeneities. Spin Echo T2 images require long TR and long TE, so they take longer to acquire than T1-weighted images (the scan time depends directly on the TR). On these scans fluids have high intensities, and water- and fat-based tissues are depicted in an intermediate grey scale. T2 images are often thought of as a map to pathology because collections of abnormal

fluid are bright against the darker normal tissue. Notice that the relationship between T2-weighted image appearance and the actual T2 value is different from the case of T1 weighting. On T2 images long T2s are brighter than short T2s, whereas on T1-weighted images long T1s are darker than short T1s.[4]

Proton Density:

Bearing in mind that the proton densities (i.e. water content) for most tissues are rather similar, you might wonder why we bother to produce PD weighted images since they will have less contrast than either T1 or T2 images. The reason is partly historical: when MRI was first used clinically, Gradient Echo images had very poor quality due to lack in hardware advances, so only SE images tended to be used. As already explained T2 weighted Spin Echo images require a long TR and they therefore take a long time to acquire. However, it is possible to create another echo at a shorter TE. This produces an image at the same slice location and within the same scan time, but with PD weighting instead of T2 weighting. So PD images did not carry any expense if you wanted a T2 image, and the dual echo sequence is still popular even though these days we can do a fast spin echo (FSE) T2 scan in a very short time.[4] Another significant reason is that in radiology an alternative contrast always carry extra information and that is always valued.

Definition of SNR in MR imaging:

As per National Electrical Manufacturers Association (NEMA) SNR is ‘‘Image SNR is a parameter that relates to clinical usefulness of magnetic resonance images and also is a sensitive measure of hardware performance. Experience has shown that variations in system calibration, gain, coil tuning, radiofrequency shielding, or other similar parameters are usually demonstrated by a corresponding change in image SNR’’. [5]

Usually in when we refer to ‘signal’ we mean the value of a pixel or voxel (voxel is a volume representation of a pixel) that is represented as brightness in the image. That is related to the NMR signal (i.e. what we measure from the coils). In any MR acquisition there is a certain amount of signal available dependent upon the MR characteristics of the tissue and the pulse sequence chosen. Since the NMR signal that is returned from the patient during the scan has to be divided amongst the voxels that make up the image, the fundamental factor influencing the size of the signal is the number of protons within each voxel. By ‘noise’ we refer to random differences in pixel values which give images a grainy, mottled look. Usually this noise originates mainly from the patient’s tissues.

In a MR image the individual voxels that make up the image will contain a mixture of signal and noise. The ratio of signal intensity in the image to noise level is the signal-to-noise ratio (SNR). Images with a poor signal to noise ratio will appear fuzzy. An important aspect of image optimization is to ensure that there is a high enough signal to noise ratio for the images to be diagnostically

useful. Low signal to noise ratio may result in missing small details or the obscuring of subtle contrast changes. [6]

Noise:

Noise comes from random variations in electrical current. So it is called electronic noise, and it exists in all electrical circuits. This obviously includes the MR coils with which we measure the signal, but it also includes the electrically conducting tissues of the patient. Human tissue contains many ions ide which act as carriers of electrical currents within the body, e.g. in nerve conduction. These currents generate varying magnetic fields which induce a noise voltage in the coil. The most effective way to reduce this noise is to use a small or dedicated anatomy coil. [6]

Quality control in MR scanners contains many aspects of operation, signal to noise ratio is in the core of the metrics that characterize the quality of a produced image. If we prove that we are able to monitor how stable a system performs by retrospectively assessing images then we are half way through and the only thing left is to automate the process and maybe incorporate this into the scanners ending up having a self-monitored system.

So in this thesis we will explore the feasibility of the previous argument. Can we retrospectively check the performance of the equipment over time through analysis of the already captured images?

Chapter 2: State-of-the-art

The signal-to-noise ratio (SNR) is a basic but broad metric for MRI system performance. Signal and noise measurement in Fourier MR imaging is a difficult task. Henkelman [7] described how signal intensity values for magnitude reconstructed MR images acquired with linear RF coils are determined in the presence of low signal to noise ratios. Gudbjartsson and Patz [8] provided a theoretical analysis of the statistical features of noise in magnitude and phase Fourier MR images (Rayleigh distribution). For estimating signal to noise ratio for phased-array RF coils, Constantinides et al [9] developed comparable noise distribution functions and correction factors.

Kaufman et al [10] proposed the single-acquisition method employed in the manual of the American College of Radiologists. However, it's important to check for artifacts in the ROI where the noise standard deviation is calculated.

Furthermore, measurements in non-uniform regions caused by bandwidth-limiting filtering, truncation of background signal data, and RF filtering of signal data at the frequency-encoding range's borders should be avoided. Some MRI system manufacturers employ an alternative technique of signal to noise ratio assessment, NEMA MS1-2008, Method 1[5], which involves taking two successive scans with identical scan settings.

Sijbers et al [11] examined the single image acquisition approach described in manual of the American College of Radiologists [12] to NEMA Method 1 and found that, except in the presence of irregular ghosting or fluid motion, NEMA Method 1 produces adequate signal to noise ratio readings. Firbank et al [13] collected data directly linking the two procedures, indicating that the single acquisition method is useful in a quality assurance program "because it is quicker and easier to implement and is a good indication of the more exact procedure." The single most crucial concept in measuring SNR, regardless of the method utilized, is reproducibility. Every time a test is run, it must be done the same way, and every time an analysis is run, it must be done the same way.

To detect slight alterations in signal to noise ratio owing to physical equipment failure, it's important to keep methodological variations to an absolutely minimal. Because the noise term is small and in the signal to noise ratio denominator, test design decisions that increase the noise measurement's accuracy are more essential over those that enhance the mean signal measurement's accuracy. It is important to note that the signal to noise ratio data reported in the annual system performance evaluation report using the methods outlined in the manual of American College of Radiologists for the quality control [12] are estimations rather than precise measurements of the true signal to noise ratio .

However, for the vast majority of devices, this is a repeatable index that suffices for routine quality control. It may be essential to adjust the signal by subtracting the background from the signal before computing the signal to noise ratio in some low-field systems when the background intensity is significant relative to the signal, something that does not apply in the circumstances under the examined data were acquired in our case.

Until now we have provided definitions of signal and noise, and we have explained the production of signal and how noise is created, as one can understand the key factor with greater impact in signal to noise ratio is the noise. In the NEMA MS 1-2008 (R2014, R2020) p.4-9 [5] one can find the four procedures to evaluate noise over an image.

This is the updated standard that it is implemented in every acceptance test performed. In that standard it is stated that, to evaluate image noise, any of four methods may be used.

The first method necessitates the subtraction of two pictures carrying signals. This approach can be used with any n-channel receive system, however it is susceptible to artifacts caused by system drift. In that standard, this approach is only applicable to single-channel receive systems.

The second method necessitates the creation of an image that is devoid of NMR signals. The noise measurement is not susceptible to system drift because it is derived directly from an image with no coherent signal, but it is prone to any process that alters the predicted noise distribution. In accordance with the scope of the standard, the correction factor defined in the standard is solely applicable to single-channel receive systems. (This technique can be implemented for any n-channel receive system with a different acceptable correction factor.) Any image reconstruction/processing approach that affects the noise characteristics of a noise-only region is incompatible with this method. According to methods 1 and 2, the second scan must be completed in fewer than 5 minutes from the finish of the first scan to the start of the second.

The third method creates two synthetic signal images from a single scan, which may then be subtracted to create a noise image. This approach can be used for any n-channel receive system, however in that standard, it is limited to single-channel receive systems. Because the effective time difference between the two derived images equals the acquisition's sample interval, this method is only slightly affected by system drift.

A single acquisition method is the fourth and final method. Outside the phantom, the noise is evaluated in a region devoid of visible signal artifacts. Because just one image is captured, it is not affected by system drift artifacts, but signal artifacts that are not visible can skew the noise statistics. It can be used for any n-channel receive system with the proper correction factors as indicated in the second technique, however in that standard, this method is limited to single-channel receive systems. Any image reconstruction/processing approach that changes the noise properties of a noise-only region is incompatible with this method. As noise in parallel imaging methods is spatially

variable, none of the methods described here are compatible with parallel imaging methods in their current state.

More comprehensively the four methods from the NEMA Standards Publication MS 1-2008 (R2014, R2020) [5] :

Method 1

The second image (image 2) is acquired under exactly the same conditions as the first. No system adjustment or calibration should be performed between scans.

a) Calculate a pixel-by-pixel difference image [referred to as (image 3) from now on] as follows:

(image 3) = (image 1) – (image 2)

b) Determine the Standard deviation SD of the pixel values within the MROI on (image 3):

$$SD = \left[\frac{\sum_{i=1}^{n} \sum_{j=1}^{m_i} \left(V(i,j) - \overline{V} \right)^2}{\sum_{i=1}^{n} (m_i) - 1} \right]^{\frac{1}{2}} \quad \text{Equation 1}$$

Where: $\overline{V}$ is the average pixel value in (image 3)

V (i,j) is the pixel value in (image 3)

i index spans the read encode direction

j index spans the phase encode direction

The MROI spans a maximum of n read points in the image and m_i denotes the variable number of phase encode points possible in a regularly shaped MROI.

c) The method of calculating the Standard deviation can affect the result. Temporal instability of the MR imager can give rise to artifacts in the subtracted image which increase the Standard deviation. These artifacts normally have low spatial frequency, and their effect on the calculation of the Standard deviation can be sharply reduced by evaluating the successive differences between the adjacent points in (image 3).

$$SD = \left[\frac{\sum_{i=1}^{n} \sum_{j=1}^{m_j - 1} (V(i, j+1) - V(i, j))^2}{2 \sum_{i=1}^{n} (m_i - 1)} \right]^{\frac{1}{2}} \quad \text{Equation 2}$$

d) Temporal stability can be evaluated by comparing the result of Equation 2 and Equation 1. In the absence of temporal instabilities, the two measures of SD should be nominally the same. With increasing temporal instability the results of both Equation 1 and Equation 2 will increase, but the results of Equation 1 will increase more rapidly. Since both measures of SD involve a difference operation [image 3], the image noise measurement must be corrected as follows:

$$\text{image noise} = \frac{SD}{\sqrt{2}} \quad \text{Equation 3}$$

Method 2:

A noise scan image is acquired with the phantom in its original position and with no RF excitation. In this situation, it is permitted to decrease TR and accelerate the noise scan acquisition. Ensure that the bandwidth, matrix size and number of signal averages are held constant. Ensure that the MR system does not automatically change other relevant parameters as a result of the above changes.

a) Ensure that the output from the transmitter is such that no NMR signal is generated upon execution of the noise scan. It shall be permitted to turn off the RF amplifier or otherwise suppress the RF excitation.
b) Ensure that the system receiver attenuation (or gain control) and any scaling of the image reconstruction are identical to that of the first scan.
c) Except for TR, the noise image is acquired under the same conditions as (image 1). No system adjustment or calibration shall be performed between the scans.
d) Determine the Standard deviation, SD, of the pixel values within the MROI on the noise image using Equation 1.
e) If a magnitude image is evaluated, the image noise will not be Gaussian distributed, but rectified to a Rician distribution. The change of noise distribution must be compensated for as the SNR measure assumes the noise is Gaussian distributed. For a single-channel system the correction factor is:

$$\text{image noise} = \frac{SD}{0.66} \qquad \text{Equation 4}$$

The factor of 0.66 $\left(\cong \sqrt{(4-\pi)/2}\right)$ accounts for the Rayleigh distribution of the noise in the magnitude [14].

Method 3:

As previously mentioned, system drift can make it difficult to calculate image noise statistics by subtracting two sequentially obtained images. As the time interval between data measurements grows longer, system drift becomes more evident. Method 3 minimizes the time between measurements to the bare minimum, effectively eliminating tainted noise statistics. This approach employs a single, special image acquisition, but the end result is the same as method 1, two signal images that are subtracted. This solution requires access to raw k-space data to be implemented.

a) Obtain an image with a read direction field of view that is double the size of the one used in Methods 1 and 2. Within that field of view, center the phantom. Double the read direction matrix size at the same time. This may be performed on some MRI machines by doubling the read and phase matrix sizes, then reducing the phase encode direction matrix size by 50% with a rectangular field of view. If feasible, keep the same bandwidth as Methods 1 and 2. If you need to keep the overall sampling time and TE the same, quadruple the acquisition bandwidth.

b) Save the raw k-space, time domain data. Introduce the following data decimation process in the read direction: split out all even number index data points in the read direction into data file 'even' and all the remaining odd number index data points in the read direction into data file 'odd' magnitude reconstruct these two decimated data sets. Since every other data point is in the same data file, the sampling rate has been cut in half and the read direction field of view size has been reduced by the same factor of two. The field of view, and number of image data points, should now equal that collected in Methods 1 and 2.

c) Now we have two images with a temporal difference that is effectively the time between sampling, there is almost no drift between them. Subtract images in the same manner as in method 1:

(image 3) = (image 1) – (image 2)

d) Calculate the signal MROI mean S in both (new image 1) and (new image 2) and average together.
e) Calculate SD in the same measurement MROI region as in step d, but in (new image 3). This is equivalent to step b. in method 1.
f) Since method 3, step c. computed the difference of images, it is necessary to divide the SD by √2. This is equivalent to step d in method 1. If the bandwidth of acquisition was doubled in step a, it is necessary to scale the results to be equivalent to method 1 and 2. In this case, divide SD by another factor of √2.
g) Optionally, the alternate Standard deviation computation (Method 1, step c) can be applied to [new image 3], but this should not be necessary.

Method 4:

As previously mentioned, system drift can make it difficult to calculate image noise statistics by subtracting two sequentially obtained images. Another option is to calculate the SNR from a reconstructed image of a single magnitude. The signal S is computed as previously, but the noise SD is calculated from a background area of the image that is well away from the phantom and free of noticeable artifacts. There are measurement concerns connected with this noise SD determination: tiny non-visible artifacts will skew the SD measurement, picture post-processing may affect the SD, and some image post-processing methods may filter out the entire background area, making the noise SD assessment impossible. Furthermore, when obtaining images at high bandwidths, the receiver sub-system frequency response may be non-uniform, resulting in distinct noise statistics on either side of the image (high positive vs low negative frequencies). As a result, the statistical measurements from the four corners should be averaged together. When utilizing this strategy, you must guarantee that certain factors are not present.

a) Compute the MROI's average pixel value. The signal S is the result of subtracting the baseline pixel offset value (if any) from the total.

b) Draw a noise MROI in the image's background, sufficiently away from the phantom and any visible artifacts. In both the read and phase directions, the noise MROI projections must be far away from the signal creating phantom. As a result of this requirement, the noise MROI is positioned in the image's corner. To give enough room for a reasonable MROI, this method may require a higher FOV than the previous methods (A minimum of 1000 points is required, however more points are preferred for more consistent outcomes).

c) There are two ways to calculate the noise SD in the MROI described in step b. Because a magnitude image is being analysed, the image noise will be rectified to a Rayleigh distribution rather than a Gaussian distribution, providing no additional bias exists. As a result, the noise SD is calculated using the Rayleigh distribution's SD or mean, appropriately corrected to the comparable predicted Gaussian distribution. For a single-channel image, if the SD of the Rayleigh distribution is measured, the correction factor is:

$$\text{image noise} = \frac{SD}{0.66} \qquad \text{Equation 6}$$

In the same manuscript in page 9 [15] the procedure for signal to noise ratio determination is described as:

$$SNR = \frac{S}{\text{image noise}} \qquad \text{Equation 7}$$

So if we combine equations 6 and 7 we end up with the so called 'practical' way for determination of signal to noise ratio.

$$SNR_{practical} = \frac{S}{SD} \times 0.66$$

Those being said one can easily understand that for MR imaging that does not use acceleration factors or fancy filtering techniques the literature is solid and there is no point trying to reinvent the wheel. But what about trying to take advantage of a wheel that has already been turned? Can we use the already acquired data to have an overview of the equipment's performance SNR wise?
If this is feasible we may have taken a step closer to an easier quality control approach that does not need equipment being reserved for measurements instead of scanning patients. One can argue that acceleration techniques will be more and more prominent in the short coming new MR imaging era. Due to constant hardware advances scan times will continue to drop allowing us to have a more forgiving approach in some cases. The tug of war between quantity and quality will never end, but it is that need that drives the changes in the MR imaging field, and quality control is the silent factor in that process.

Chapter 3: Research methodology

A brevit description of the measuring process is the following:

''Measurements of SNR taken over specific areas of standard brain MRI examination in a longitudinal time period of thirty six months is implemented in this study. Data will originate from those already existed in the MRI system database or the general hospital database Picture Archiving and Communication System (PACS). T2 weighted MR images from the routine referred patients' brain MRI examination protocol will be used.

Signal will be obtained from Regions Of Interest (ROIs) of standard anatomical structures positioned axial head scans. Noise will be obtained from artifact free ROIs positioned at selected area outside the depicted images. The final SNR for each patient will be obtained as an average from the ratio of Signals vs Noises utilizing the aforementioned ROIs. The practical SNR method described in the AAPM protocol will be used. SNR data will be collected and tabulated for a total period of thirty six months. SNR measurements reproducibility and repeatability figures like %CV will be then calculated. The robustness of the clinical brain examination protocol, in terms of SNR, for the specific MRI system will be finally assessed.

Signal to Noise Ratio (SNR) measurements in clinical MRI is a straight forward quality metric for the assessment of the diagnostic quality of an MRI image. Signal to noise ratio is mostly related to all functional parameters of the MRI system as well as to the type and special characteristics of the specific MRI examination performed.

Measurements of signal to noise ratio taken from nine specific areas over standard brain MRI examination in a longitudinal time period of thirty six months will be performed in this study.

Although the three year span may seem too big it was selected for various reasons:

a) We wanted a large enough period of time to observe for system behavioural drift.
b) We wanted a large enough sample tank to collect a sufficient group of data due to our knowledge that not all images would be eligible for analysis.

We should always keep in mind that MR imaging department of the University Hospital in Heraklion serves a population close to one million (Crete and Dodecanese islands complex and part of Cyclades islands complex) and is the only University Imaging department meaning a high load of pathologies are being imaged due to the surveying character the department has .

An initial inspection of the data base revealed that two days of the week dominated in routine brain protocol appearances, Tuesdays and Thursdays. So after including these days only every week we

were led to a huge data set that would not be manageable, in order to keep the time period as big as possible and the data set big enough but manageable sampling rate was altered. Sampling was performed every other week.

After sampling rate adaptation was applied the data pool consisted of 2050 exams (2018: 684, 2019:763, and 2020: 603). After exclusion factors were applied only 492 exams where selected.

Exclusion factors was decided to be:

a) Examinee age smaller than 15 years (Children population is always examined separately in medical sciences)
b) Existence of any kind of pathology in the areas under inspection.
c) Existence of any kind of artifacts in the areas under inspection.
d) Poor image quality as a result of poor cooperation of the examinee.

In quality control protocols a spin echo T1 weighted image is used for acquiring the needed data. The purpose of this sequence selection is to keep scan time as small as possible. Remember the repetition time, phase encoding stages, and number of averages all contribute to the acquisition time for a traditional spin echo (TR x phase steps x NEX). With a one-second TR, 128 phase steps, and two averages, the acquisition time would be approximately 1 x 128 x 2 = 256 seconds, or 4 minutes and 16 seconds.[16] Since TR values in T1 imaging are smaller than T2 imaging thus scan time will be less.

In our case this does not apply because the data have already been acquired. We should keep in mind that human brain is not even remotely as uniform as the phantoms used in the aforementioned practice. In T1 weighted imaging as already explained we record signals from significantly less nuclei over T2 weighted imaging. So in non-uniform samples it will be easier to observe signal variations in T2 than in T1 imaging. Having this in mind the selection of T2 imaging was made.

In clinical T2 weighted imaging classic spin echo has been substituted with Fast Spin Echo (FSE) sequences due to the fact that the outcome is almost the same but in much less time, this is feasible due to the fact that in FSE imaging we exploit the advanced hardware (which came at later time and not since the begging) and create more encoding steps in one repetition time thus recording the same signal in faster mode simplistically speaking.

Axial orientation of the slices was selected for the following reasons:

a) For non-medical personnel anatomy is better perceived in this plane making it less error prone to work with.
b) Diameter of the head in coronal plane is smaller thus having less area to spread the ROI's.

c) Sagittal plane would give as almost the same maximum diameter, depending the angulation used during the prescription of the slices (parallel to genu and splenium of corpus callosum or true axial) but it would not allow us to evaluate for inhomogeneities of right over left side.
d) Usually axial level prescription does not require attention to the slightest detail thus it is performed in the first stages of the exam and even claustrophobic patients have a better cooperation level leading to better image quality.

Noise will be obtained from artifact free ROI positioned outside the depicted images at a posterior level (as SNR1).

Signal will be obtained from Regions Of Interest (ROIs) of standard anatomical structures positioned in axial head scans. These areas will be:

a) Skin fat in the right and left occipital area (as SNR2 and SNR6 accordingly)
b) Posterior lateral horn of the right and left ventricle (as SNR3 and SNR7 accordingly)
c) Area of right and left Thalamus of the brain (as SNR4 and SNR8 accordingly)
d) Area of the right and left lateral area of Superior frontal gyrus (as SNR5 and SNR9 accordingly)

The selection of placing ROIs in both right and left side was made to allow us to evaluate any possible fluctuation in signal recordings in both sides of the coil.

Skin fat area was selected due to the small variation in signal strength coming from that area. Fat in the occipital area exists in the vast majority of people and it is positioned close to the edge of the coil allowing us to check for posterior edge homogeneity.

Ventricles of the brain are positioned close to the center of the coil and produce high signal due to the CSF inside them creating an environment where pathology detection is relatively is easy thus making eligibility decision and center coil homogeneity check easier.

Thalamus area is included in the most significant areas of the brain and also is one of the most homogeneous areas if not pathological. High or low signal areas are easily recognised and its central position allows center coil homogeneity check.

Lateral area of the superior frontal gyrus is positioned in the anterior edge of the brain and thus close to the anterior edge of the coil allowing us to check for anterior edge homogeneity.

The process of image evaluation and ROI drawing and placement will be performed on EVORAD PACS-HIS system of the University Hospital of Heraklion. (Version 4.10) [17]

Platform was selected due to its user friendly environment and most importantly due to its ability to export measurement values in spreadsheet files, allowing us to build our database easier.

ROIs were drawn once and recreated by copying and pasting them in the desired area giving us the advantage of recreating the same size of ROI over and over again. After this will be performed data will be exported and tabulated in a single file.

Statistical analysis will be performed through MedCalc software version 15.2.2 .[18]

The final signal to noise ratio for each patient will be obtained as an average from the ratio of Signals vs Noise utilizing the aforementioned ROIs. The practical signal to noise ratio method described in the AAPM protocol will be used.

Coefficient of Variation will be calculated by dividing the standard deviation of each measurement by the mean value of each measurement. This will allow us to make comparisons of the different datasets although the datasets refer to different areas .[19]

The datasets will be assessed for normal distribution and comparisons will be made through independent sampling T-test (Smirvov-Kolmogorov test & Mann Whitney test) .

Finally the robustness of the clinical brain examination protocol, in terms of SNR, for the specific MRI system will be finally assessed.

Chapter 4: Research findings / results

After sampling rate adaptation was applied the data pool consisted of 2050 exams (2018: 684, 2019:763, and 2020: 603). After exclusion factors were applied only 492 exams where selected.

The sample was consisted of 311 exams performed on females and 181 on males.Female participants consisted the 63.2% of the total examinees with minimum age of 15 years and maximum age of 83 years and with a mean age of 47,9 years. The standard deviation of the age in the female population was calculated at 15,7 years of age. Male participants consisted the 36.8% of the total examinees with minimum age of 16 years and maximum age of 81 years and with a mean age of 36.8 years. The standard deviation of the age in the male population was calculated at 17,4 years of age.

Analytic statistics will be presented in the form of tables for easier comprehension.

Female Population	
Mean Age	47,9
Min Age	15
Max Age	83
SD of Age	15,7
Percentage of Female examinees	63,2
Total count	311
Total examinees	492

Table 3.Female population statistics

Male Population	
Mean Age	36,8
Min Age	16
Max Age	81
SD of Age	17,4
Percentage of Male examinees	36,8
Total count	181
Total examinees	492

Table 4. Male population statistics

CV% of SNR Values summary statistics table

	N	Minimum	Maximum	Mean	Median	SD	RSD	25 - 75 P
FSNR2	311	32,400	92,000	63,285	63,000	8,7550	0,1383	58,550 to 68,650
FSNR6	311	5,200	88,800	62,968	62,800	9,1985	0,1461	58,100 to 68,200
FSNR3	311	45,200	107,700	81,279	80,500	9,5104	0,1170	76,200 to 85,950
FSNR7	311	47,100	108,700	80,996	80,600	9,3203	0,1151	76,000 to 85,500
FSNR4	311	15,800	38,600	26,002	26,150	3,7773	0,1453	24,000 to 28,100
FSNR8	311	15,900	37,900	25,853	25,800	3,7291	0,1442	23,950 to 28,050
FSNR5	311	11,900	34,400	20,441	20,100	3,3985	0,1663	18,600 to 22,150
FSNR9	311	12,300	35,900	20,756	20,400	3,5431	0,1707	18,800 to 22,600
MSNR2	181	22,990	84,300	52,324	52,750	10,2544	0,1960	45,145 to 59,095
MSNR6	181	21,600	76,100	52,175	52,600	10,1255	0,1941	45,300 to 58,550
MSNR3	181	47,410	102,770	75,541	75,275	10,1736	0,1347	69,090 to 81,880
MSNR7	181	47,300	96,900	75,181	74,800	10,0131	0,1332	69,400 to 81,150
MSNR4	181	15,000	33,900	23,977	23,850	3,6136	0,1507	21,600 to 26,500

MSNR8	181	15,100	33,900	23,843	23,650	3,4352	0,1441	21,550 to 26,200
MSNR5	181	11,400	38,600	18,954	18,800	3,3249	0,1754	16,800 to 20,700
MSNR9	181	11,400	30,700	19,352	18,900	3,2796	0,1695	16,950 to 21,100

Table 5. Statistical summary table referring to SNR values measured in all areas of the complete data pool.

Variable	FSNR2
Sample size	312
Lowest value	32,4000
Highest value	92,0000
Arithmetic mean	63,2849
95% CI for the Arithmetic mean	62,3097 to 64,2602
Median	63,0000
95% CI for the median	62,1000 to 64,1000
Variance	76,6498
Standard deviation	8,7550
Relative standard deviation	0,1383 (13,83%)
Standard error of the mean	0,4957
Coefficient of Skewness	-0,09918 (P=0,4676)
Coefficient of Kurtosis	1,0685 (P=0,0045)
Kolmogorov-Smirnov test[a] for Normal distribution	D=0,0513 reject Normality (P=0,0463)

[a] Lilliefors significance correction

Percentiles		95% Confidence interval
2,5	44,6900	39,1431 to 47,8531
5	48,8600	45,6224 to 50,4288
10	52,6700	49,9444 to 54,6319
25	58,5500	57,3526 to 59,6712
75	68,6500	67,0000 to 69,9237
90	74,1600	72,0000 to 76,3834
95	77,7900	75,2892 to 79,0950
97,5	80,7100	78,4363 to 85,4606

Table 6.Kolmogorov-Smirnov test report for normal distribution of SNR values in females in area of skin fat in left occipital area in women.

Variable	FSNR3
Sample size	312
Lowest value	45,2000
Highest value	107,7000
Arithmetic mean	81,2785
95% CI for the Arithmetic mean	80,2191 to 82,3379
Median	80,5000
95% CI for the median	79,9203 to 81,5000
Variance	90,4485
Standard deviation	9,5104
Relative standard deviation	0,1170 (11,70%)
Standard error of the mean	0,5384
Coefficient of Skewness	-0,1249 (P=0,3612)
Coefficient of Kurtosis	1,6476 (P=0,0002)
Kolmogorov-Smirnov test[a] for Normal distribution	D=0,0717 reject Normality (P=0,0005)

[a] Lilliefors significance correction

Percentiles		95% Confidence interval
2,5	60,0700	51,3323 to 65,5062
5	67,8600	60,7050 to 70,0072
10	71,4400	69,1889 to 72,7879
25	76,2000	75,3763 to 77,3712
75	85,9500	85,0000 to 87,3237
90	93,9200	90,5560 to 95,9000
95	98,4900	95,5964 to 102,3503
97,5	102,8200	98,8894 to 107,0000

Table 7.Kolmogorov-Smirnov test report for normal distribution of SNR values in females in area of left posterior lateral horn of the ventricles .

Variable	FSNR4

Sample size	312
Lowest value	15,8000
Highest value	38,6000
Arithmetic mean	26,0016
95% CI for the Arithmetic mean	25,5808 to 26,4224
Median	26,1500
95% CI for the median	25,6203 to 26,4000
Variance	14,2677
Standard deviation	3,7773
Relative standard deviation	0,1453 (14,53%)
Standard error of the mean	0,2138
Coefficient of Skewness	0,1207 (P=0,3774)
Coefficient of Kurtosis	0,7670 (P=0,0240)
Kolmogorov-Smirnov test[a] for Normal distribution	D=0,0619 reject Normality (P=0,0059)

[a] Lilliefors significance correction

Percentiles		95% Confidence interval
2,5	18,2900	16,5286 to 19,0000
5	19,0200	18,5050 to 20,3000
10	21,0400	19,8000 to 22,0440
25	24,0000	23,5000 to 24,4000
75	28,1000	27,5000 to 28,5000
90	30,2300	29,6560 to 31,5667
95	32,7800	31,0964 to 34,6876
97,5	34,7000	32,8000 to 36,5946

Table 8.Kolmogorov-Smirnov test report for normal distribution of SNR values in females in are of left thalamus.

Variable	FSNR5

Sample size	312
Lowest value	11,9000
Highest value	34,4000
Arithmetic mean	20,4407
95% CI for the Arithmetic mean	20,0621 to 20,8193
Median	20,1000
95% CI for the median	19,7000 to 20,4797
Variance	11,5497
Standard deviation	3,3985
Relative standard deviation	0,1663 (16,63%)
Standard error of the mean	0,1924
Coefficient of Skewness	0,8628 (P<0,0001)
Coefficient of Kurtosis	2,3512 (P<0,0001)
Kolmogorov-Smirnov test[a] for Normal distribution	D=0,0732 reject Normality (P=0,0004)

[a] Lilliefors significance correction

Percentiles		95% Confidence interval
2,5	14,5000	13,3411 to 14,7000
5	14,9200	14,5025 to 15,8000
10	16,3000	15,4722 to 17,3440
25	18,6000	18,2000 to 18,9000
75	22,1500	21,7000 to 22,7237
90	24,1600	23,5000 to 25,1556
95	26,1900	24,9000 to 28,7000
97,5	28,7700	26,2000 to 32,0768

Table 9.Kolmogorov-Smirnov test report for normal distribution of SNR values in females in area of left lateral superior frontal gyrus.

Variable	FSNR6

Sample size	312
Lowest value	5,2000
Highest value	88,8000
Arithmetic mean	62,9683
95% CI for the Arithmetic mean	61,9436 to 63,9929
Median	62,8000
95% CI for the median	62,0000 to 63,9797
Variance	84,6123
Standard deviation	9,1985
Relative standard deviation	0,1461 (14,61%)
Standard error of the mean	0,5208
Coefficient of Skewness	-0,8629 (P<0,0001)
Coefficient of Kurtosis	5,2260 (P<0,0001)
Kolmogorov-Smirnov test[a] for Normal distribution	D=0,0691 reject Normality (P=0,0011)

[a] Lilliefors significance correction

Percentiles		95% Confidence interval
2,5	44,0000	35,5912 to 48,0318
5	48,7100	45,4224 to 51,4000
10	53,2000	50,0722 to 55,0000
25	58,1000	57,1000 to 59,2712
75	68,2000	67,0288 to 69,2710
90	73,6300	71,9000 to 75,4389
95	77,6000	75,1928 to 81,6975
97,5	81,7700	77,7894 to 84,7714

Table 10.Kolmogorov-Smirnov test report for normal distribution of SNR values in females in area of skin fat in right occipital area.

Variable	FSNR7

Sample size	312
Lowest value	47,1000
Highest value	108,7000
Arithmetic mean	80,9955
95% CI for the Arithmetic mean	79,9573 to 82,0337
Median	80,6000
95% CI for the median	79,8203 to 81,6000
Variance	86,8687
Standard deviation	9,3203
Relative standard deviation	0,1151 (11,51%)
Standard error of the mean	0,5277
Coefficient of Skewness	-0,1186 (P=0,3855)
Coefficient of Kurtosis	1,5754 (P=0,0003)
Kolmogorov-Smirnov test[a] for Normal distribution	D=0,0676 reject Normality (P=0,0015)

[a] Lilliefors significance correction

Percentiles		95% Confidence interval
2,5	59,9300	51,8572 to 65,3168
5	66,6500	60,0174 to 69,8036
10	71,3700	69,2333 to 72,4440
25	76,0000	74,9526 to 76,8712
75	85,5000	84,6000 to 87,5000
90	92,8300	90,1681 to 95,2556
95	97,0300	94,9748 to 100,3975
97,5	101,3800	97,5682 to 106,0178

Table 11.Kolmogorov-Smirnov test report for normal distribution of SNR values in females in area of skin fat in area of right posterior lateral horn of the ventricles .

Variable	FSNR8

Sample size	312
Lowest value	15,9000
Highest value	37,9000
Arithmetic mean	25,8532
95% CI for the Arithmetic mean	25,4378 to 26,2686
Median	25,8000
95% CI for the median	25,4000 to 26,3000
Variance	13,9065
Standard deviation	3,7291
Relative standard deviation	0,1442 (14,42%)
Standard error of the mean	0,2111
Coefficient of Skewness	0,08483 (P=0,5342)
Coefficient of Kurtosis	0,6819 (P=0,0381)
Kolmogorov-Smirnov test[a] for Normal distribution	D=0,0602 reject Normality (P=0,0084)

[a] Lilliefors significance correction

Percentiles		95% Confidence interval
2,5	18,1300	16,5697 to 18,9106
5	19,0100	18,2075 to 19,9036
10	20,8700	19,7722 to 22,2440
25	23,9500	23,3000 to 24,3000
75	28,0500	27,4000 to 28,6237
90	30,3000	29,6000 to 31,1667
95	32,1900	30,9000 to 33,5000
97,5	34,3400	32,3894 to 35,6000

Table 12.Kolmogorov-Smirnov test report for normal distribution of SNR values in females in area of right thalamus.

Variable	FSNR9

Sample size	312
Lowest value	12,3000
Highest value	35,9000
Arithmetic mean	20,7564
95% CI for the Arithmetic mean	20,3617 to 21,1511
Median	20,4000
95% CI for the median	20,1000 to 20,8000
Variance	12,5533
Standard deviation	3,5431
Relative standard deviation	0,1707 (17,07%)
Standard error of the mean	0,2006
Coefficient of Skewness	0,9107 (P<0,0001)
Coefficient of Kurtosis	2,5421 (P<0,0001)
Kolmogorov-Smirnov test[a] for Normal distribution	D=0,0822 reject Normality (P<0,0001)

[a] Lilliefors significance correction

Percentiles		95% Confidence interval
2,5	14,4300	13,4822 to 14,7106
5	15,0100	14,5025 to 15,9036
10	16,3700	15,5722 to 17,4440
25	18,8000	18,5000 to 19,1712
75	22,6000	22,0288 to 23,0237
90	24,7300	23,7000 to 25,8278
95	26,8700	25,5892 to 28,9901
97,5	30,1200	27,2788 to 32,5125

Table 13.Kolmogorov-Smirnov test report for normal distribution of SNR values in females in area of right lateral superior frontal gyrus.

Variable	MSNR2

Sample size	180
Lowest value	22,9900
Highest value	84,3000
Arithmetic mean	52,3236
95% CI for the Arithmetic mean	50,8153 to 53,8318
Median	52,7500
95% CI for the median	50,5769 to 54,8652
Variance	105,1532
Standard deviation	10,2544
Relative standard deviation	0,1960 (19,60%)
Standard error of the mean	0,7643
Coefficient of Skewness	-0,09476 (P=0,5939)
Coefficient of Kurtosis	0,09773 (P=0,6712)
Kolmogorov-Smirnov test[a] for Normal distribution	D=0,0387 accept Normality (P>0.10)

[a] Lilliefors significance correction

Percentiles		95% Confidence interval
2,5	30,7300	24,3507 to 36,9300
5	36,9350	29,4487 to 38,6112
10	39,5300	37,6892 to 41,6174
25	45,1450	42,5763 to 46,8709
75	59,0950	58,2593 to 61,0876
90	65,1000	62,9172 to 67,3633
95	68,8150	65,5515 to 71,3613
97,5	71,1900	68,8231 to 80,5092

Table 14.Kolmogorov-Smirnov test report for normal distribution of SNR values in males in area of skin fat in left occipital area.

Variable	MSNR2

Back-transformed after logarithmic transformation.

Sample size	180
Lowest value	22,9900
Highest value	84,3000
Geometric mean	51,2535
95% CI for the Geometric mean	49,6999 to 52,8558
Median	52,7500
95% CI for the median	50,5769 to 54,8652
Coefficient of Skewness	-0,8023 (P=0,0001)
Coefficient of Kurtosis	1,2462 (P=0,0116)
Kolmogorov-Smirnov test[a] for Normal distribution	D=0,0721 reject Normality (P=0,0236)

[a] Lilliefors significance correction

Percentiles		95% Confidence interval
2,5	30,7300	24,3018 to 36,9279
5	36,9329	29,4393 to 38,6112
10	39,5300	37,6892 to 41,6174
25	45,1450	42,5748 to 46,8708
75	59,0946	58,2592 to 61,0876
90	65,0999	62,9162 to 67,3631
95	68,8121	65,5514 to 71,3613
97,5	71,1900	68,8202 to 80,3919

Table 15.Back-transformed after logarithmic transformation Kolmogorov-Smirnov test report for normal distribution of SNR values in males in area of skin fat in left occipital area.

Variable	MSNR3

Sample size	180
Lowest value	47,4100
Highest value	102,7700
Arithmetic mean	75,5414
95% CI for the Arithmetic mean	74,0451 to 77,0378
Median	75,2750
95% CI for the median	73,6456 to 76,2000
Variance	103,5025
Standard deviation	10,1736
Relative standard deviation	0,1347 (13,47%)
Standard error of the mean	0,7583
Coefficient of Skewness	0,01620 (P=0,9272)
Coefficient of Kurtosis	0,2889 (P=0,3714)
Kolmogorov-Smirnov test[a] for Normal distribution	D=0,0668 reject Normality (P=0,0489)

[a] Lilliefors significance correction

Percentiles		95% Confidence interval
2,5	55,5300	47,4578 to 58,5446
5	58,5500	52,8482 to 63,5104
10	64,1650	59,0904 to 65,5211
25	69,0900	67,6599 to 70,3866
75	81,8800	80,1742 to 84,6766
90	89,1900	86,3885 to 91,5202
95	92,7750	89,9140 to 96,9647
97,5	96,9200	92,7783 to 102,1657

Table 16.Kolmogorov-Smirnov test report for normal distribution of SNR values in males in area of left posterior lateral horn of the ventricles.

Variable	MSNR4

Sample size	180
Lowest value	15,0000
Highest value	33,9000
Arithmetic mean	23,9772
95% CI for the Arithmetic mean	23,4457 to 24,5087
Median	23,8500
95% CI for the median	23,3000 to 24,7000
Variance	13,0577
Standard deviation	3,6136
Relative standard deviation	0,1507 (15,07%)
Standard error of the mean	0,2693
Coefficient of Skewness	0,1315 (P=0,4602)
Coefficient of Kurtosis	0,1765 (P=0,5310)
Kolmogorov-Smirnov test[a] for Normal distribution	D=0,0308 accept Normality (P>0.10)

[a] Lilliefors significance correction

Percentiles		95% Confidence interval
2,5	16,8000	15,0435 to 18,3000
5	18,3000	16,2785 to 19,0612
10	19,4500	18,8000 to 20,2735
25	21,6000	20,8494 to 22,2102
75	26,5000	25,5000 to 27,0000
90	28,3500	27,4530 to 29,7792
95	30,1500	28,8388 to 32,3490
97,5	32,2000	30,1506 to 33,7261

Table 17.Kolmogorov-Smirnov test report for normal distribution of SNR values in males in are of left thalamus.

Variable	MSNR5

Sample size	180
Lowest value	11,4000
Highest value	38,6000
Arithmetic mean	18,9539
95% CI for the Arithmetic mean	18,4649 to 19,4429
Median	18,8000
95% CI for the median	18,2000 to 19,1631
Variance	11,0549
Standard deviation	3,3249
Relative standard deviation	0,1754 (17,54%)
Standard error of the mean	0,2478
Coefficient of Skewness	1,2299 (P<0,0001)
Coefficient of Kurtosis	5,9003 (P<0,0001)
Kolmogorov-Smirnov test[a] for Normal distribution	D=0,0824 reject Normality (P=0,0046)

[a] Lilliefors significance correction

Percentiles		95% Confidence interval
2,5	13,5000	11,4000 to 14,3000
5	14,3000	13,1275 to 14,9000
10	15,2000	14,4030 to 16,0000
25	16,8000	16,2373 to 17,3102
75	20,7000	19,9000 to 21,7627
90	23,2000	22,5000 to 24,0000
95	24,2000	23,5388 to 25,6704
97,5	25,0000	24,2013 to 33,5137

Table 18.Kolmogorov-Smirnov test report for normal distribution of SNR values in males in area of left lateral superior frontal gyrus.

Variable	MSNR6

Sample size	180
Lowest value	21,6000
Highest value	76,1000
Arithmetic mean	52,1750
95% CI for the Arithmetic mean	50,6857 to 53,6643
Median	52,6000
95% CI for the median	50,1000 to 54,8000
Variance	102,5259
Standard deviation	10,1255
Relative standard deviation	0,1941 (19,41%)
Standard error of the mean	0,7547
Coefficient of Skewness	-0,1758 (P=0,3247)
Coefficient of Kurtosis	-0,1393 (P=0,7848)
Kolmogorov-Smirnov test[a] for Normal distribution	D=0,0437 accept Normality (P>0.10)

[a] Lilliefors significance correction

Percentiles		95% Confidence interval
2,5	30,4000	23,8171 to 36,1911
5	36,2000	29,6551 to 38,7224
10	40,0000	37,6030 to 41,4735
25	45,3000	42,2000 to 47,2205
75	58,5500	56,8000 to 61,4013
90	65,8000	64,0265 to 67,6941
95	68,0500	66,5388 to 71,3235
97,5	71,1000	68,0519 to 74,3611

Table 19.Kolmogorov-Smirnov test report for normal distribution of SNR values in males in area of skin fat in right occipital area.

Variable	MSNR6

Back-transformed after logarithmic transformation.

Sample size	180
Lowest value	21,6000
Highest value	76,1000
Geometric mean	51,1206
95% CI for the Geometric mean	49,5774 to 52,7118
Median	52,5976
95% CI for the median	50,1000 to 54,8000
Coefficient of Skewness	-0,8607 (P<0,0001)
Coefficient of Kurtosis	1,4220 (P=0,0061)
Kolmogorov-Smirnov test[a] for Normal distribution	D=0,0759 reject Normality (P=0,0133)

[a] Lilliefors significance correction

Percentiles		95% Confidence interval
2,5	30,4000	23,6850 to 36,1843
5	36,1932	29,6519 to 38,7223
10	39,9999	37,6030 to 41,4735
25	45,3000	42,2000 to 47,2204
75	58,5498	56,8000 to 61,4000
90	65,7999	64,0265 to 67,6941
95	68,0498	66,5388 to 71,3234
97,5	71,1000	68,0517 to 74,3345

Table 20. Back-transformed after logarithmic transformation Kolmogorov-Smirnov test report for normal distribution of SNR values in males in area of skin fat in right occipital area.

Variable	MSNR7

Sample size	180
Lowest value	47,3000
Highest value	96,9000
Arithmetic mean	75,1811
95% CI for the Arithmetic mean	73,7084 to 76,6538
Median	74,8000
95% CI for the median	72,9369 to 76,1000
Variance	100,2618
Standard deviation	10,0131
Relative standard deviation	0,1332 (13,32%)
Standard error of the mean	0,7463
Coefficient of Skewness	-0,06743 (P=0,7041)
Coefficient of Kurtosis	0,1111 (P=0,6457)
Kolmogorov-Smirnov test[a] for Normal distribution	D=0,0495 accept Normality (P>0.10)

[a] Lilliefors significance correction

Percentiles		95% Confidence interval
2,5	55,2000	47,3869 to 59,1962
5	59,2000	52,8162 to 62,1672
10	63,4000	59,9059 to 64,9000
25	69,4000	67,5120 to 71,0000
75	81,1500	78,9795 to 84,0133
90	89,1500	86,6325 to 92,3703
95	92,6000	90,6104 to 96,3449
97,5	95,6000	92,6013 to 96,7696

Table 21. Kolmogorov-Smirnov test report for normal distribution of SNR values in males in area of skin fat in area of right posterior lateral horn of the ventricle.

Variable	MSNR8

Sample size	180
Lowest value	15,1000
Highest value	33,9000
Arithmetic mean	23,8428
95% CI for the Arithmetic mean	23,3375 to 24,3480
Median	23,6500
95% CI for the median	23,3000 to 24,3000
Variance	11,8009
Standard deviation	3,4352
Relative standard deviation	0,1441 (14,41%)
Standard error of the mean	0,2560
Coefficient of Skewness	0,1309 (P=0,4622)
Coefficient of Kurtosis	0,1280 (P=0,6145)
Kolmogorov-Smirnov test[a] for Normal distribution	D=0,0419 accept Normality (P>0.10)

[a] Lilliefors significance correction

Percentiles		95% Confidence interval
2,5	17,2000	15,4043 to 18,0975
5	18,1000	16,9020 to 19,1000
10	19,4500	18,4148 to 20,0000
25	21,5500	20,9747 to 22,2307
75	26,2000	25,4898 to 26,9000
90	28,1000	27,3000 to 28,9911
95	29,6500	28,2388 to 30,9745
97,5	30,9000	29,6519 to 33,5957

Table 22. Kolmogorov-Smirnov test report for normal distribution of SNR values in males in area of right thalamus.

Variable	MSNR8

Back-transformed after logarithmic transformation.

Sample size	180
Lowest value	15,1000
Highest value	33,9000
Geometric mean	23,5932
95% CI for the Geometric mean	23,0899 to 24,1074
Median	23,6499
95% CI for the median	23,3000 to 24,3000
Coefficient of Skewness	-0,3192 (P=0,0780)
Coefficient of Kurtosis	0,1934 (P=0,5040)
Kolmogorov-Smirnov test[a] for Normal distribution	D=0,0684 reject Normality (P=0,0393)

[a] Lilliefors significance correction

Percentiles		95% Confidence interval
2,5	17,2000	15,4004 to 18,0963
5	18,0989	16,9011 to 19,1000
10	19,4499	18,4146 to 20,0000
25	21,5499	20,9745 to 22,2305
75	26,2000	25,4897 to 26,9000
90	28,0998	27,3000 to 28,9911
95	29,6496	28,2388 to 30,9745
97,5	30,9000	29,6515 to 33,5939

Table 23. Back-transformed after logarithmic transformation Kolmogorov-Smirnov test report for normal distribution of SNR values in males in area of right thalamus.

Variable	MSNR9

Sample size	180
Lowest value	11,4000
Highest value	30,7000
Arithmetic mean	19,3517
95% CI for the Arithmetic mean	18,8693 to 19,8340
Median	18,9000
95% CI for the median	18,3369 to 19,5892
Variance	10,7555
Standard deviation	3,2796
Relative standard deviation	0,1695 (16,95%)
Standard error of the mean	0,2444
Coefficient of Skewness	0,4832 (P=0,0093)
Coefficient of Kurtosis	0,5375 (P=0,1575)
Kolmogorov-Smirnov test[a] for Normal distribution	D=0,0684 reject Normality (P=0,0391)

[a] Lilliefors significance correction

Percentiles		95% Confidence interval
2,5	13,8000	11,4869 to 14,3987
5	14,4000	13,6510 to 15,1612
10	15,4500	14,5030 to 16,2735
25	16,9500	16,5373 to 17,9000
75	21,1000	20,4898 to 22,4000
90	23,8500	22,7795 to 24,7881
95	24,9500	24,0164 to 27,0235
97,5	26,8000	24,9519 to 29,8305

Table 24. Kolmogorov-Smirnov test report for normal distribution of SNR values in males in area of right lateral superior frontal gyrus.

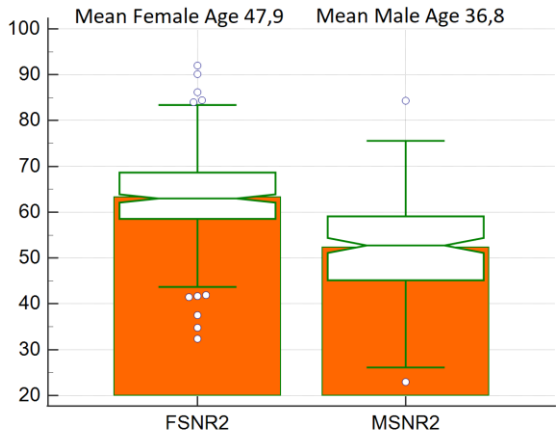

Figure 1. Correlation of SNR values in area of skin fat in left occipital area in women over men.

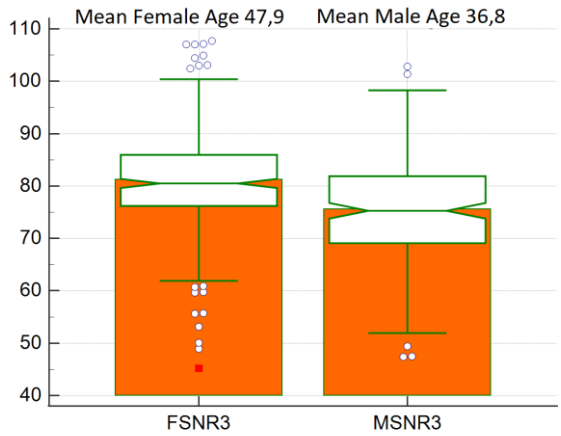

Figure 2. Correlation of SNR values in area of left posterior lateral horn of the ventricle in women over men.

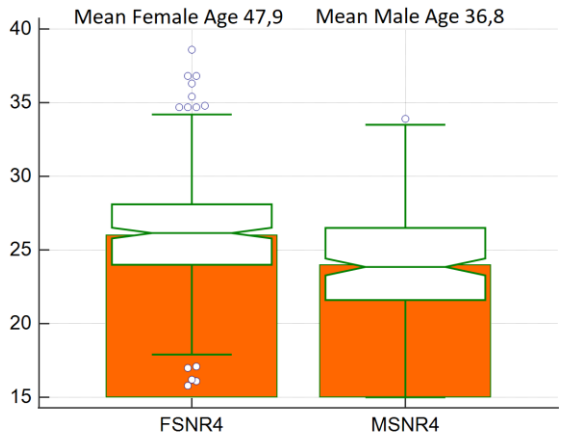

Figure 3. Correlation of SNR values in area of left thalamus in women over men.

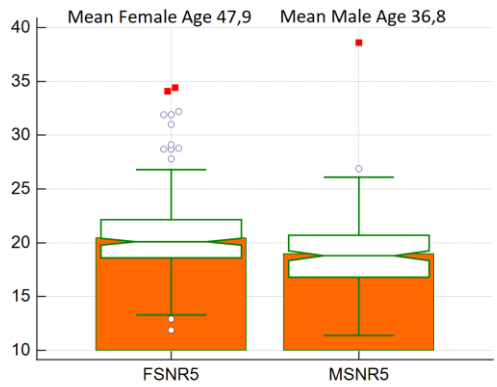

Figure 4. Correlation of SNR values in area of left lateral superior frontal gyrus in women over men.

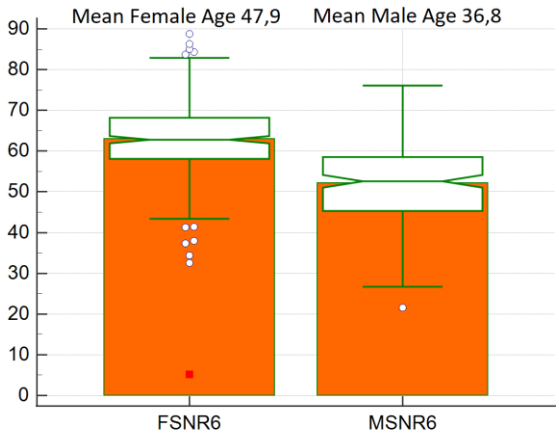

Figure 5.Correlation of SNR values in area of skin fat in right occipital area in women over men.

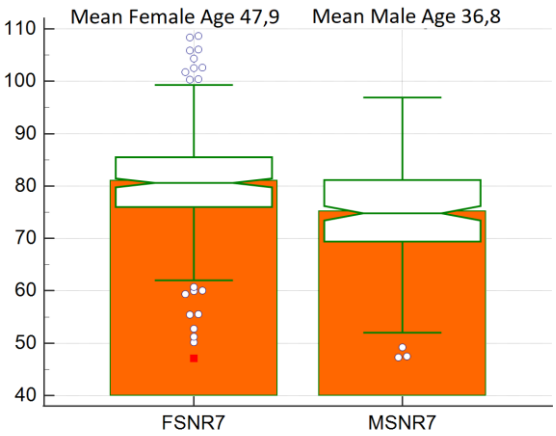

Figure 6.Correlation of SNR values in area of right posterior lateral horn of the ventricles in women over men.

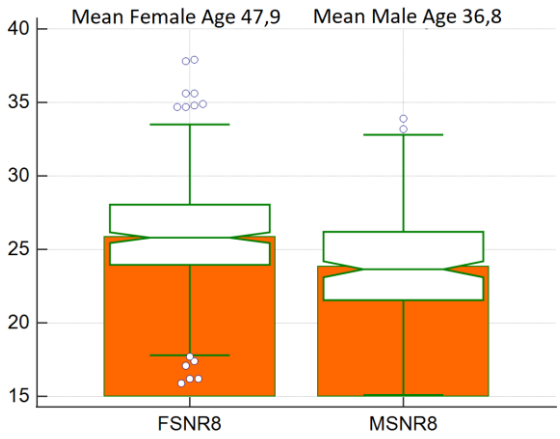

Figure 7. Correlation of SNR values in area of right thalamus in women over men.

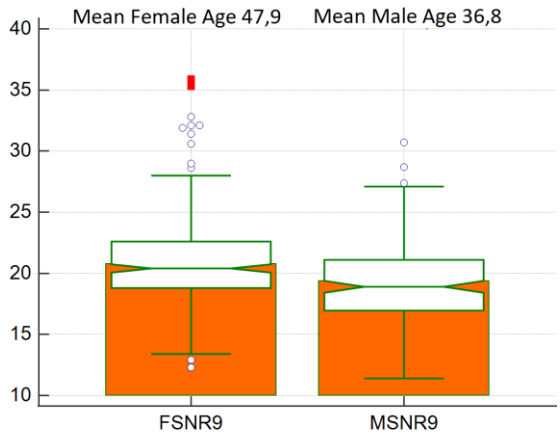

Figure 8. Correlation of SNR values in area of right lateral superior frontal gyrus in women over men.

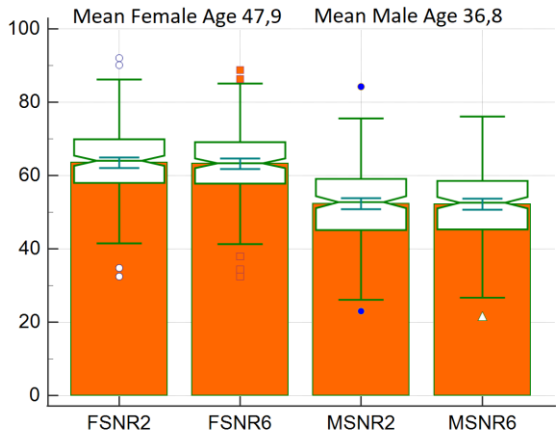

Figure 9. Correlation of SNR values in right and left area of skin fat in occipital area in women over men.

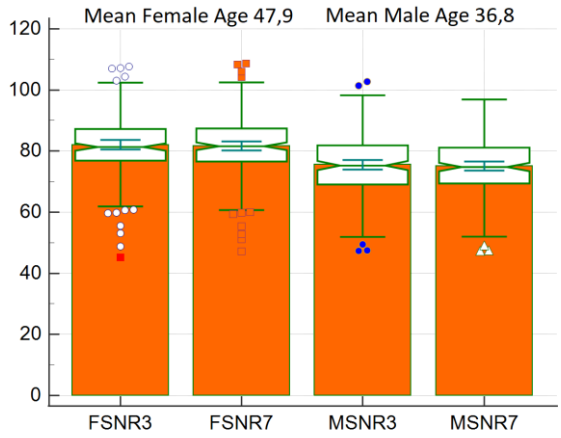

Figure 10. Correlation of SNR values in right and left area of posterior lateral horn of the ventricles in women over men.

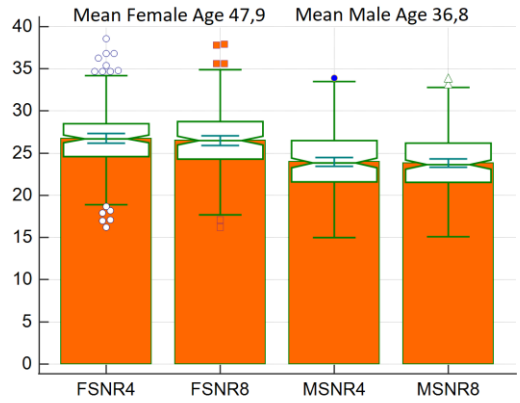

Figure 11. Correlation of SNR values in right and left area of thalamus in women over men.

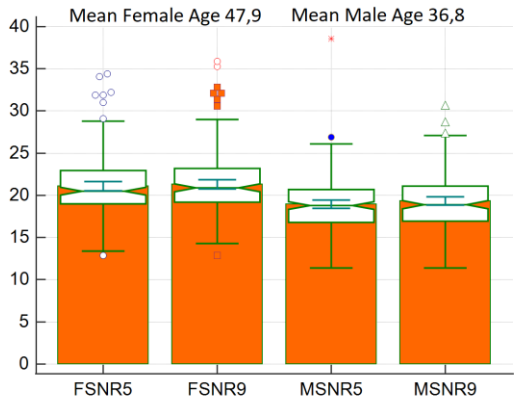

Figure 12. Correlation of SNR values in right and left area of lateral superior frontal gyrus in women over men.

Chapter 5: Discussion and analysis of findings

As shown by the tables presented in the previous chapter (Tables 6 -24) datasets underwent thorough analysis via Kolmogorov-Smirnov test in order to characterize their dispersion and use the appropriate statistical method to compare them.

In these tests P-values received where less than 0.05,resulting in a non-Normal dispersion , meaning the sample cannot accurately be described by arithmetic mean and standard deviation, and samples should not be submitted to any parametrical statistical test or procedure, such as e.g. a t-test.

The Mann-Whitney test is the non-parametric equivalent of the independent t-test.This test should be used when the sample data are not Normally distributed, and they cannot be transformed to a Normal distribution by means of a logarithmic transformation.

In females data showed non normal distribution in all of the nine areas of measurement.

In males data showed non normal distribution predominately. Areas with normal distribution of data underwent back transformation after logarithmic transformation. If the data shows outliers at the high end, a logarithmic transformation can sometimes help. The logarithm function tends to squeeze together the larger values in the data set and stretches out the smaller values that was the purpose of using it.

Due to the non-normal distribution of the data sets , Mann – Whitney test was applied through MedCalc software [18] in order to compare the SNR values of the different areas.

Analytical presentation of the statistical characteristics is shown in table 5 , variables show similar statistical behaviour ,meaning that SNR values had no significant variation. (Remember that we refer in left right pairs e.g. SNR2- SNR6 refer to skin fat ROIs, SNR3-SNR7 to ventricular ROIs, SNR4-SNR8 in Thalamus ROIs,SNR5-SNR9 in frontal gyrus ROIs). Given the fact that through the exclusion factors we were led in a sample with a homogenous image pattern if statistical analysis revealed any inconsistencies between right and left side that would be due to equipment instability.

In the figures displayed in the previous chapter (Figures 1-12) one can notice an elevated signal intensity in females over males in all areas, this is attributed to the higher mean age of the female sample resulting in more CSF present in the brain tissue due to normal ageing. Overall statistical analysis showed no evidence inconsistencies in the recorded values and the performance of the equipment is characterized as stable in terms of SNR.

Chapter 6: Conclusion and recommendations

During this thesis we investigated the behaviour, over time, of the equipment used in clinical MR imaging at the facilities of University hospital of Heraklion, through multiple series of repetitive measurements on clinical MR images that have already been captured during exams that were performed over a three year span (2018-2020) in the solely MR scanner of the University hospital of Heraklion in order to prove that monitoring , in terms of SNR performance, is feasible by retrospectively assessing image data in a non-pathological dataset.

After extensive analysis of the data set it is clear that non pathological datasets can result in a viable alternative for monitoring the performance of a system in terms of SNR. This was depicted in the graphical representations of SNR measurements throughout the process with the tight relevance of the SNR-pair values and the consistent measurements received in both left and right side of the measured area . Meaning that SNR measuring process could be potentially replaced by the already acquired dataset if the dataset is cautiously prepared and the SNR measurement ROIs are placed consistently.

During this research only four hundred and ninety two exams where eligible out of the two thousand and fifty exams that fell into the period under inspection. A larger dataset would be beneficiary to the credibility of the process. Another potential issue might be the age difference between male and female samples. So a more balanced dataset in the perspective of age and gender participants would eliminate any doubts regading dataset imbalances affecting the end result.
Another area that one could deepen and enrich is the statistical manipulation of the dataset, a more sophisticated analysis would strengthen the end result.

Restrospective analysis of already acquired datasets could provide the desired outcomes in terms of SNR performance monitoring if done properly. With the constant forward leaping of the technology in pattern recognition and the advances in artificial intelligence there is a potential for developing self-monitored systems without any intervention.

References

[1] Yeung, J., Murphy, A. Repetition time. Reference article, Radiopaedia.org. https://radiopaedia.org/articles/14588

[2] Yeung, J., Jones, J. Echo time. Reference article, Radiopaedia.org. https://doi.org/10.53347/rID-14587

[3] Prabhakar, G., Murphy, A. Flip angle. Reference article, Radiopaedia.org. https://doi.org/10.53347/rID-45465 https://radiopaedia.org/articles/45465

[4] Mc Robbie, D., Moore, E., Graves, M., & Prince, M. (2006). Seeing is believing: Introduction to image contrast. In MRI from Picture to Proton (pp. 30-46). Cambridge: Cambridge University Press. doi:10.1017/CBO9780511545405.003

[5] NEMA Standards Publication MS 1-2008 (R2014, R2020)

[6] Mc Robbie, D., Moore, E., Graves, M., & Prince, M. (2006). What you set is what you get: Basic image optimization. In MRI from Picture to Proton (pp. 65-78). Cambridge: Cambridge University Press. doi:10.1017/CBO9780511545405.005

[7] Henkelman RM. Measurement of signal intensities in the presence of noise in MR images [published correction appears in Medical Physics. 1986;13:544]. Medical Physics. 1984;12:232-233.

[8] Gudbjartsson H, Patz S. The Rician noise distribution of noisy MRI data. Magnetic Resonance in Medicine. 1995;34:910-914.

[9] Constantinides CD, Atalar E, McVeigh ER. Signal-to-noise measurements from magnitude images in NMR phased-arrays. Magnetic Resonance in Medicine. 1997;38:852-857.

[10] Kaufman L, Kramer DM, Crooks LE, Ortendahl DA. Measuring signal-to-noise ratios in MR imaging. Radiology. 1989;173:265-267.

[11]Sijbers J, den Dekker AJ, van Audekerke J, Verhoye M, van Dyck D. Estimation of the noise in magnitude MR images. Magnetic Resonance Imaging. 1998;16:87-90.

[12] American College of Radiologists 2015 Quality Control manual. https://www.acr.org/-/media/ACR/Files/Clinical-Resources/QC-Manuals/MR_QCManual.pdf

[13] Firbank MJ, Coulthard A, Harrison RM, Williams ED. A comparison of two methods for measuring the signal-to-noise ratio on MR images. Physics in Medicine and Biology. 1999;44:N261-N264.

[14] Henkelman, R. M. 1985, Medical Physics, 12, 232-233.

[15] NEMA Standards Publication MS 1-2008 (R2014, R2020) chapter (2.3.3) p.9

[16] Ballinger, J., Murphy, A. Acquisition time. Reference article, Radiopaedia.org. https://doi.org/10.53347/rID-2255

[17] http://www.evorad.com/en/products

[18] MedCalc® Statistical Software version 15.2.2 (MedCalc Software Ltd, Ostend, Belgium; https://www.medcalc.org; 2022)

[19] https://en.wikipedia.org/wiki/Coefficient_of_variation